ASPS Conference Proceedings 1: 1: 659-671 (2022)

Proceedings of

12th Structural Engineering Convention-An International Event (SEC 2022)

Available at https://asps-journals.com/index.php/acp

Seismic Performance of Irregular Building with different Variable sliding isolators and Semi active Dampers

Ajay Sharma [1, *] and Sudhir Soni[2]

[1] Professor,Dept. of Structural Engineering, MBM Engineering College, Jodhpur corresponding author (Email: ajayvidyanand@gmail.com)
[2]Ph.D. Scholar; Dept. of Structural Engineering, MBM Engineering College, Jodhpur

Paper ID - 060180

Abstract

The comparative performances of semiactive friction and stiffness dampers with different control laws in the base-isolated Irregular building subjected to bi-directionally acting strong earthquakes have been studied. The Irregular building is hybridly isolated with rubber bearings and friction pendulum system (FPS) or variable frequency pendulum isolator (VFPI) or variable curvature friction pendulum system (VCFPS). The shear type base-isolated Irregular building is modeled as three-dimensional linear elastic structure having three degrees-of-freedom at each floor level. Time domain dynamic analysis of the building has been carried out with the help of constant average acceleration Newmark-Beta method and non-linear isolation forces has been taken care by fourth-order Runge-Kutta method. The effects of variation of characteristic properties of semiactive dampers on their hysteresis loops and on the structural response of Irregular building is studied through parametric study. Comparative performances of different semiactive dampers with sliding isolation systems for seismic control of Irregular building have been observed through time history plots and peak response performance indices. It has been found that semiactive electromagnetic friction damper work efficiently with VFPI and VCFPS in comparison FPS for the Irregular building for near field earthquakes as it not only reduces base displacement at lower control force but also give lower base shear and story drift in base-isolated Irregular building. The control laws based on modulated homogeneous friction control semiactive friction dampers better than the predictive control law.

Key Words: Base isolation; VFPI; VCFPS; semiactive friction damper; resetting semiactive stiffness damper; modulated homogeneous friction controller.

1. INTRODUCTION

In recent past *base isolation* has been proved as a most widely accepted and implemented seismic protection system for buildings, bridges and liquid storage structures. Base isolation, isolate the structure from ground shaking effectively from the frequency range in which the structure is highly susceptible of getting damaged or over-strained. The motif is to lower the floor acceleration and inter story drifts to limit the probable damage to the structure and its contents in simple and cost-effective manner (Buckle and Mayes 1990; Jangid and Dutta 1995; Kelly 1986). Base isolation does improve the superstructure seismic response but gives large base displacement especially when the structure is subjected to near-field earthquakes. The ground motion of near-field earthquakes is characterized by high peak acceleration and high velocity pulse with a long period component as well as large peak displacement. Such characteristics are responsible for severe damages to urban infrastructures, including buildings, bridges, lifeline systems, etc. The large isolator displacement of isolators under near-fault ground motions needs to be controlled without inordinate cut-off in the structural performance as many researchers are of the opinion that base-isolated buildings can be vulnerable to the large pulse-like ground motions generated at near-fault locations (Hall *et al.*, 1995; Heaton *et al.*, 1995). Also, the strict code provisions regarding base-isolated buildings for accommodating large isolator displacements and larger Maximum capable earthquakes (MCEs) require the need of additional control. Application of conventional nonlinear isolators like Friction pendulum system (FPS) or lead rubber bearings restricts the base displacement but worsen the superstructure response. Though recent improvement in FPS developed some variable curvature sliding isolators like variable frequency pendulum isolator (VFPI) and variable curvature friction pendulum system (VCFPS) which give better seismic response but with larger isolator displacement. Thus, base isolation in such situation may not provide adequate protection against such earthquakes so applications of some additional control devices are required. These additional control devices reduce large isolator displacement, but at the expense of significant increases in inter-storey drift and floor acceleration in the superstructure. The additional

*Corresponding author. Tel: +918813971517; E-mail address: ajayvidyanand@gmail.com

Published online: December 19, 2022
doi:10.38208/acp.v1.567

control devices can be based on passive, active and semiactive control. Passive control devices like passive viscous or friction dampers though do not require external power but due to their constant characteristic response to highly varying earthquake loading limit their performance, thus they may fail to achieve desired level of control. Active control devices require huge source of power supply for their electro-hydraulic or electromechanical actuator which may not available constantly in the event of catastrophe. On one hand the occurrence of earthquakes in the designed life of structures may not be quite frequent and on other hand the stability and robustness of active controllers are yet to be established thus employment and maintenance of such control devices can be unfeasible. In such situations application of semiactive control devices is suitable solution as they are not only robust and reliable as passive controllers but devoid of ills of active controllers also.

A semi-active control device (or semiactive damper) generally developed from a passive control system which has been subsequently controlled to allow for maneuvering of mechanical properties. For example, supplemental energy dissipation devices which dissipate energy through shearing of viscous fluid, orificing of fluid, and sliding friction have been modified to behave in a semi-active manner. The mechanical properties of these systems can be adjusted based on feedback from the excitation and/or from the measured response. As in an active control system, a controller monitors the feedback measurements and generates an appropriate command signal for the semi-active devices. The control forces are developed through appropriate (based on a pre-determined control algorithm) adjustment of the mechanical properties of the semi-active control system. Furthermore, the control forces in many semi-active control systems primarily act to oppose the motion of the structural system and therefore promote the global stability of the structure. Semiactive control systems generally require a small amount of external power for operation (on the order of tens of watts). Several researchers worked on such semi active devices and their controlling algorithms for improving the seismic response of structures along with reduction in base displacement.

Passive base isolation when clubbed with semiactive control devices is known as “Smart base isolation”. Semiactive friction dampers, semiactive stiffness dampers and semiactive fluid dampers are some common semiactive control devices in which effective “controlled variation” is exercised on frictional force, stiffness and viscous damping respectively. Semiactive friction dampers are effective for longer duration due to less degradation due to ageing and insensitive to temperature changes. Resetting semiactive stiffness dampers (RSASD) are also effective semiactive control devices in which a spring and resetting device can be realized through pressurized gas and some gas valves. The resetting releases the accumulated vibration energy captured and stored in the stiffness part of the damper, and allows the damper to dissipate more vibration energy in each cycle of motion. Although due to the action of resetting, the RSASD damper inevitably introduces an abrupt change of the damper force at each moment when the damper is reset which brings in exciting higher structural acceleration response, else it is found to be very effective in suppressing the displacement response.

The present study investigate the effectiveness of comparative performances of different semiactive friction and stiffness dampers and control laws for seismic control of base-isolated Irregular building (Narasimhan *et al.*, 2006) which is bi-directionally acted upon by strong near field earthquakes and isolated with FPS or VFPI or VCFPS. The specific objectives of the study are (i) to investigate the influence of variation of characteristic quantities of different semiactive dampers on the response of base-isolated Irregular building through a parametric study (ii) to study the influence of variation of characteristic quantities of different semiactive dampers on their force displacement relationships and (iii) to investigate the comparative performance of base-isolated Irregular building isolated with sliding isolators with different semiactive dampers.

2. PROBLEM FORMULATION

2.1 Base-Isolated Irregular Building

The asymmetric base-isolated Irregular building is eight-storied steel-braced framed, 82.4m long and 54.3m wide (Narasimhan *et al.*, 2006). The bearing level plan of the L-shaped asymmetric building is shown in Figure 1(a). The superstructure bracing is located at the building perimeter. Metal decking and a grid of steel beams support all rigid concrete floor slabs. The steel superstructure is supported on a reinforced concrete base slab, which is integral with concrete beams below, and drop panels below each column location. The isolators are connected between these drop panels and the footings below. The superstructure is modeled as a three-dimensional linear elastic shear structure. Floor slabs and the base mat are assumed to be rigid in plane. The superstructure and the base are modeled using three master degrees of freedom (DOF) per floor at the center of mass. The combined model of the superstructure (24 DOF) and isolation system (3 DOF) consists of total 27 DOF. All twenty-four modes in the fixed-base case are used in modeling the superstructure. The superstructure damping ratio is assumed to be 5 percent in all fixed-base modes. The isolation system consists of 92 isolators and an additional 16 semiactive dampers located as shown in the Figure 1 (a).

The three-dimensional dynamic analysis of the base-isolated Irregular building is carried out considering superstructure condensed linear-elastic, as for base-isolated buildings superstructures can be considered remain elastic.

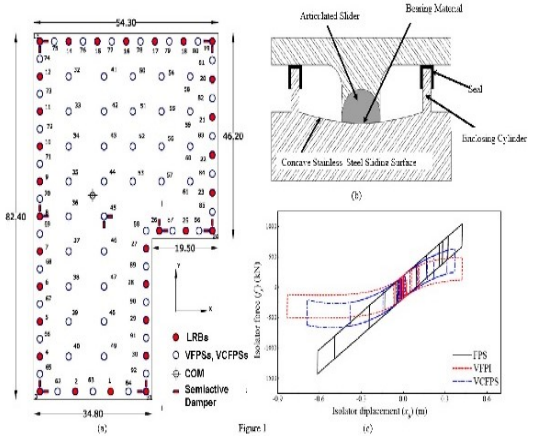

Figure 1

Figure 1 (a) Bearing level plan of base-isolated Irregular building; (b) schematic diagram of variable curvature sliding isolator and (c) Force-displacement diagram of VFPI, VCFPS and FPS isolators.

The equations of motion are developed in such a way that the fixed-base properties are used for modeling the linear superstructure. The non-linear isolation bearing is modeled explicitly using the discrete biaxial Bouc–Wen model and the forces in the bearings are transformed to the center of mass of the base using a rigid base slab assumption. All the isolation bearings can be modeled individually or globally by equivalent lumped elements at the center of mass of the base. The equations of motion for the elastic superstructure are expressed in the following matrix form

$$M\ddot{U} + C\dot{U} + KU = -MR_{inf}\left(\ddot{U}_g + \ddot{U}_b\right) \quad (1)$$

where M is the superstructure lumped mass matrix of size 24×24; C is the superstructure damping matrix of size 24×24 in the fixed-base case; K is the superstructure stiffness matrix of size 24×24 in the fixed-base; R_{inf} is the matrix of earthquake influence coefficients of size 24×3; $\ddot{U}$, $\dot{U}$ and U represent the floor acceleration, velocity and displacement vectors relative to the base respectively of size 24×1; $\ddot{U}_b$ is the vector of base accelerations relative to the ground of size 3×1; and $\ddot{U}_g$ is the vector of ground accelerations of size 3×1.

The equation of motion of base mass can also be written as

$$R'_{inf}M\left[\ddot{U} + R_{inf}\left(\ddot{U}_g + \ddot{U}_b\right)\right] + M_b\left(\ddot{U}_g + \ddot{U}_b\right) + f_b + f_c = 0 \quad \ldots. (2)$$

in which M_b is the diagonal mass matrix of the rigid base of size 3×3 and f_b is the vector containing the cumulative bearing forces transferred by all 92 isolators and f_c is the vector containing the cumulative controller forces due to 16 semiactive dampers at the centre of base mass of size 3×1.

The overall governing equation of motion of complete structure can be written by combining equations (1) and (2), as

$$\begin{bmatrix} M & MR_{inf} \\ R'_{inf}M & R'_{inf}MR_{inf}+M_b \end{bmatrix}\begin{Bmatrix}\ddot{U}\\ \ddot{U}_b\end{Bmatrix} + \begin{bmatrix} C & 0 \\ 0 & 0 \end{bmatrix}\begin{Bmatrix}\dot{U}\\ \dot{U}_b\end{Bmatrix} + \begin{bmatrix} K & 0 \\ 0 & 0 \end{bmatrix}\begin{Bmatrix}U\\ U_b\end{Bmatrix} + \begin{Bmatrix}0\\ f_b\end{Bmatrix} + \begin{Bmatrix}0\\ f_c\end{Bmatrix} \quad \ldots. (3)$$
$$= -\begin{bmatrix} MR_{inf} \\ R'_{inf}MR_{inf}+M_b \end{bmatrix}\{\ddot{U}_g\}$$

The equation (3) is solved using Newmark-Beta unconditionally stable constant-average acceleration method and nonlinear forces generated by isolators are updated using Runge-Kutta Fourth order method.

2.2 Isolation Systems

In this study the base-isolated Irregular building is isolated by 31 laminated rubber bearings (ERBs) and 61 either FPS or VFPI or VCFPS isolators *i.e.* total 92 isolators (Refer Figure 1(a)). The force vector f_b contains the algebraic sum of the forces produced by these isolators at the centre of mass of the base mat in x and y directions and torsional moment produced due to them.

The forces $f_x$and f_y, produced by the ERB in x and y directions respectively, can be expressed as

$$f_x = c_b v_{bx} + k_b x_b \quad \ldots \quad (4)$$

$$f_y = c_b v_{by} + k_b y_b \quad \ldots. (5)$$

where c_b and k_b are the damping and horizontal stiffness of the bearing; $v_{bx,}$ v_{by} and $x_{b,}$ y_b are velocities and displacements of bearing in x and y directions respectively. The horizontal stiffness and damping of the bearing are governed by isolation time period and damping ratio of the isolation system. The fundamental period of isolation system consisting ERBs and sliding isolators is 3 sec. The characteristic damping ratio (ζ) of ERB is kept 0.06.

The isolator forces offered by FPS can be expressedas

$$f_x = k_b x_b + \mu w z_x \quad \ldots. (6)$$

$$f_y = k_b y_b + \mu w z_y \quad \ldots. (7)$$

where w is the weight supported by the FPS; μ is coefficient of friction between the sliding surfaces taken as 0.06; f_x and $f_y$is the isolator force offered by the FPS in x and y directions respectively. Jangid [2005] showed that the frictional forces of sliding system presented by both conventional and hysteretic models yielded similar seismic response for the isolated structures. Thus, in the present study, the frictional forces are modelled hysteretically using the Bouc-Wen Model. z_x and z_y are the hysteretic coefficients and can be derived from Bouc-Wen equation, which is expressed as

$$U^Y\begin{Bmatrix}\dot{z}_x\\ \dot{z}_y\end{Bmatrix} = \alpha\begin{Bmatrix}\dot{x}_b\\ \dot{y}_b\end{Bmatrix} - \begin{bmatrix} z^2{}_x\left(\gamma\,\mathrm{sgn}\left(\dot{x}_b z_x\right)+\beta\right) & z_x z_y\left(\gamma\,\mathrm{sgn}\left(\dot{y}_b z_y\right)+\beta\right) \\ z_x z_y\left(\gamma\,\mathrm{sgn}\left(\dot{x}_b z_x\right)+\beta\right) & z^2{}_y\left(\gamma\,\mathrm{sgn}\left(\dot{y}_b z_y\right)+\beta\right) \end{bmatrix}\begin{Bmatrix}\dot{x}_b\\ \dot{y}_b\end{Bmatrix} \quad \ldots. (8)$$

where $\dot{x}_b$, $\dot{y}_b$ are the isolator velocities in x and y directions respectively. U^Y is the yield displacement (0.305 mm) and the parameters α, β and γ control the shape of the loop and are selected such that predicted response from the model closely matches the experimental results. For the present study, the values of α, β and γ are taken 1, 0.9 and 0.1 respectively.

Pranesh and Sinha (Pranesh and Sinha, 2000; 2004) have developed VFPI; its radius of curvature increases upon increasing isolator displacement thus at larger isolator displacement, flatter curvature modifies the restoring force component to lower values. The isolator forces, f_x and f_y offered by the VFPI in x and y directions, respectively can be expressed as

$$f_x = k_b(z_b)x_b + \mu w z_x \quad \ldots. (9)$$

$$f_y = k_b(z_b)y_b + \mu w z_y \quad \ldots. (10)$$

where $k_b(z_b)$ is the instantaneous stiffness depends upon the displacement dependent radius of curvature of sliding surface which is constant in case of FPS. The details regarding instantaneous stiffness and relevant terms can be obtained from the above cited references. The force-deformation diagram of the VFPI shown in Figure 1 (c) in dotted red, manifest that at larger isolator displacements under strong earthquakes, lower values of isolator force reflect better structural response.

VCFPS developed by Tsai *et al.*, (2003; 2005) has the mechanical outlook which is very much similar to that of the FPS. The difference between the VCFPS and FPS is that the radii of curvature of the VCFPS can be lengthened with an increase of the isolator displacement similar to VFPI. The change in radii of curvature can alter the fundamental period of the base-isolated structure and sway it away from the predominant periods of near-fault ground motions, and the resonant possibility of the superstructure with earthquakes can be avoided. The isolator forces, f_x and f_y offered by the VCFPS in x and y directions, respectively similarly

calculated as Equations (9) and (10) by taking $k_b(z_b)$ the instantaneous stiffness of the VCFPS in radial direction. The details regarding instantaneous stiffness and relevant terms can similarly be obtained from the above cited references. The force-displacement diagram shown in dash-dotted blue (refer Figure 1(c)) offers very mild isolator force at large displacements and thus provides better structural performance at large isolator displacements.

3. SEMIACTIVE DAMPERS AND CONTROL STRATEGIES

The present study investigates the effectiveness of following semiactive friction and stiffness dampers in curbing the large isolator displacement especially of VFPI and VCFPS and its impact on the structural response.

3.1 Predictive controlled Semiactive friction damper

In normal passive friction dampers, the frictional force is constant due to constant normal force thus during the earthquake period there shall be stick and slip states of the dampers. A friction damper is able to dissipate energy only if the damper is in its slip state. During an earthquake, the energy dissipated by a friction damper is proportional to the damper slip force; therefore, a friction damper may not be efficient if the level of the slip force is set too low and if it is too high than it will be stiff and may not slip for most of the earthquake duration. The other disadvantage due to continuous stick and slip switching, there will be unwanted high frequency structural responses (Lu 2004).

Lu (2004) developed a semi-active friction damper which is able to adjust its slip force by controlling its clamping force in real-time in response to a structure's motion during an earthquake such that it always remains in slip state. The semiactive friction damper utilizes the control named predictive control. In this control algorithm, by predicting the critical friction force which is minimum for keeping the semi-active friction damper in stick state, the method is able to produce a slip force that is only slightly lower than the critical force and constantly keeps the semi-active damper in its slip state throughout an earthquake, so the motion of the structure can be smoothly reduced. In state-space approach, if the dynamic equation of a structure can be written as

$$\dot{z}(t) = A z(t) + B u(t) + E w(t) \quad \ldots. (11)$$

where the vectors $z(t)$ and $\dot{z}(t)$ are state and first order derivative of state of the structure; u (t) denotes the vector of the controllable friction forces provided by the semi-active friction dampers; $w(t)$ is the vector of ground accelerations; A denotes the system matrix that is composed of the structural mass, damping and stiffness matrices; and B and E represent the distributing matrices of the control forces and the excitations, respectively. The force vector u (t) depends not only on the damper properties (the friction coefficient, time-varying clamping forces and dampers stiffness, etc.), but also on the structural dynamic response and can be expressed as

$$u_i(t) = \alpha[k_{d(i)}\{z_{d(i)}(t) - z_{d(i)}(t-1)\} + u_i(t-1)] \ldots. (12)$$

where for the "i^{th}" damper, $z_{d(i)}(t)$ and $z_{d(i)}(t\text{-}1)$ are the semiactive friction damper displacements at time step "t" and just previous time step (t-1); $k_{d(i)}$ is the stiffness of the damper, $u_i(t)$ and $u_i(t\text{-}1)$ are the forces offered by the semiactive friction damper at time step "t" and just previous time step (t-1) and; α is the multiplier by which the minimum force required for stick state shall be reduced to keep damper continuously in slip state. From the equation (12) it is clear that force required by the semiactive damper is a function of damper displacements and damper force at previous time step only thus no complicated sensor measurements are needed to estimate the force. The time-dependent control force is realized in the semiactive friction damper by keeping the $N_i(t)$, the clamping force as time dependent which can be calculated as

$$N_i(t) = u_i(t) / \mu \quad \ldots. (13)$$

3.2 Modulated Homogeneous Friction controlled Semiactive electromagnetic friction damper

The modulated homogeneous friction control algorithm (Inaudi 1997) is a collocated dynamic feedback law which uses the deformation of the damper as the only feedback signal to define the contact force $N_i(t)$ of the semi-active friction damper, which can be mathematically expressed as

$$N_i(t) = \beta \left| P[\Delta(t)] \right| \quad \ldots. (14)$$

where β is the positive gain coefficient with units as stiffness and $P[\Delta(t)]$ operator can be defined as

$P[\Delta(t)] = \Delta(t-s)$ where

$$s = \{\min x \geq 0 : \frac{d\Delta}{dt}(t-x) = 0\} \ldots.(15)$$

and such that Δ(t-s) is a local peak of the deformation signal.

Agrawal and Yang (2000) proposed a new semiactive electromagnetic friction damper (SAEMFD) based on the regulation of the friction force across the damper using an electromagnetic field. In most of the semiactive friction damper devices proposed and investigated in the past, use clamping mechanisms to vary the normal force across the plates. As a result, the maximum normal force is limited by the type of mechanical devices, and the clamping action may involve a time-delay. On the other hand, the normal force in the SAEMFD device can be varied simply by a regulation of currents in solenoids across the damper without a significant time-delay (Yang and Agrawal 2002; He *et al.,* 2003). Based on the above control law, He *et al*., (2003) propose three control strategies which not only can keep the semiactive friction dampers continuously in slip state but also eliminate the undesirable high frequency input inform of acceleration spikes due to switching from stick to slip states by introducing boundary layers.

According to control law known as "Discontinuous semiactive friction controller" (DSAFC) the control force can be defined as

$$u_i(t) = \begin{cases} \mu\beta \left| P[\Delta(t)] \right| \mathrm{sgn}(\dot{x}) & if \quad abs(\dot{x}) > 0 \\ 0 & if \quad (\dot{x}) = 0 \end{cases}$$

$\ldots.$ (16)

However, the DSAF controller in Equation (16) induces high frequency components due to abrupt switching and chattering around $\dot{x} = 0$, resulting in spikes in the acceleration response. The abovementioned problem can be taken care by introducing a boundary layer δ around $\dot{x} = 0$.

This control law referred as "Linear boundary layer semiactive friction controller" (LBLSAFC).

$$u_i(t) = \begin{cases} \mu\beta \left|P[\Delta(t)]\right| \text{sgn}(\dot{x}) & if \quad abs(\dot{x}) > \delta \\ \dfrac{\mu\beta \left|P[\Delta(t)]\right| \text{sgn}(\dot{x}) |\dot{x}|}{\delta} & if \quad abs(\dot{x}) \le \delta \end{cases} \quad \ldots. (17)$$

It has been observed that the performance of the controller in Equation (17) may be sensitive to the boundary layer parameter δ for a particular earthquake. This sensitivity can be reduced by modeling the linear boundary layer in Equation (17) as a smoother boundary layer using the hyperbolic function *tanh* ($\alpha \dot{x}$), where $\alpha$is a parameter representing the measure of the thickness of the boundary layer. This control law called as "Smooth boundary layer semi active friction controller" (SBLSAFC)

$$u_i(t) = \mu\beta \left|P[\Delta(t)]\right| \tanh(\alpha\dot{x}) \quad \ldots. (18)$$

3.3 Resetting semiactive stiffness damper

Resetting semiactive stiffness damper is basically a hydraulic damper which consists of a cylinder–piston system with an on–off valve in the bypass pipe connecting two sides of the cylinder filled with hydraulic oil.The effectively control of the RSASD, Yang et al. [2000] derived a general resetting control law based on the Lyapunov theory, which resets the RSASD stiffness at each moment when the relative velocity cross the damper reaches zero. When the valve is closed, the damper serves as a stiffness element with an effective stiffness $k_d$provided by the bulk modulus of the fluid inside. In the resetting mode, the value is pulsed to open and then closed quickly at appropriate time instants. Since the valve is closed most of the time, the energy is stored in the form of potential energy of the compressed oil in the damper system. At appropriate time instants, the value is opened to quickly release the energy. At this instant, the piston of the damper is reset to a new position. The control force in the damper is expressed as

$$u_i(t) = k_d(x - x_p) \quad \ldots. (19)$$

where k_d is effective damper stiffness; x is the damper displacement and x_p is the previous piston position at the instant of resetting. The semiactive damper is reset at when velocity is zero. In this resetting stiffness damper, damper stiffness is added whenever valve is closed.

4. NUMERICAL STUDY

The time domain dynamic analysis has been conducted on the computational model of base-isolated Irregular building to investigate the role of comparative performances of the different semiactive dampers and isolation systems comprising FPS or VFPI and VCFPS isolators in controlling the seismic response of the base-isolated Irregular building. The Irregular building is acted upon by seven strong earthquake ground motions acting bi-directionally in the horizontal directions ignoring vertical component of ground motions. The historical earthquakes which are used, are the 1994 Northridge *Newhall* Station (360 as Fault-Normal and 90 as Fault-Parallel); 1994 Northridge *Sylmar* Station (360 as Fault-Normal and 90 as Fault-Parallel); 1940 Imperial Valley-*El Centro* Array # 9 (180 as Fault-Normal component and 270 as Fault-Parallel component); 1994 Northridge *Rinaldi* Station (228 as Fault-Normal and 318 as Fault-Parallel); 1995 *Kobe*-JMA Station (KJM 000 component as Fault-Normal and KJM 90 component as Fault-Parallel), 1999 Taiwan *Jiji* TCU 068 station (N as Fault-Normal and W as Fault-Parallel) and 1995 *Erzincan* (Turkey) (NS as Fault-Normal and EW as Fault-Parallel). The Modified earthquake time histories of above earthquakes with time step 0.001 sec for 30 sec are used for the present study. All the earthquake ground motions are applied bi-directionally to the building, in which the fault normal component is applied in *x*-direction and fault parallel component is applied in *y*-direction.

The present study is divided in two parts. In the first part, the effects of parametric variations of characteristic quantities of the semiactive dampers on their force-displacement responses and impacts on the performance indices of the structural response are investigated to understand their role in improvement in seismic control. In the second part the comparative seismic responses of the base-isolated Irregular building are studied to control large isolator displacements of FPS or VFPI and VCFPS, by adding different semiactive dampers to the structure. The time histories and peak response criteria of absolute floor accelerations; base displacements; story drifts and base shears of the Irregular building are recorded to compare the effectiveness of the different semiactive dampers to curb large isolator displacements of the VFPI and VCFPS. The seismic response has been studied in the form of performance evaluation criteria, which are J_1 = Peak base shear of base-isolated Irregular building/corresponding value of non-isolated Irregular building; J_2 = Peak story shear of base-isolated Irregular building/corresponding value of non-isolated Irregular building; J_3 = Peak base displacement of base-isolated Irregular building; J_4= Peak story drift of base-isolated Irregular building/corresponding value of non-isolated Irregular building; J_5 = Peak absolute acceleration of base-isolated Irregular building/corresponding value of non-isolated Irregular building; J_6 = Peak Control force at the centre of base mat of base-isolated Irregular building/total weight of the Irregular building; J_7 = Root mean square (RMS) base displacement of base-isolated Irregular building ; J_8 = Root mean square (RMS) absolute acceleration of base-isolated Irregular building/corresponding value of non-isolated Irregular building; J_9 =Total energy absorbed by the semiactive dampers/ input energy and J_{10} =Maximum cumulative control force/ maximum cumulative isolator force.

In the above performance evaluation criteria, the structural response quantities are normalised by their corresponding non-isolated/ fixed base values in comparison to isolated values as in case of the base-isolated Irregular building, because the present study aims to evaluate the relative performance of different isolation systems and semiactive dampers absolutely.

4.1 Study of effects of parametric variations of characteristics of semiactive dampers on their force-displacement relationship and structural response of the Irregular building

The efficiency of any damper depends upon its energy dissipation capability which is usually manifested by their force-displacement curves or hysteresis loops. The hysteresis loops of a semiactive damper basically depend upon the control algorithm as well as on their mechanical

characteristics. The variations in the characteristic values not only modify their force deformation relationship but also the structural response. Figure 2 shows the variations of performance indices on the variation of damper stiffness.

The value of α kept equal to 0.999 so as to keep value the sliding force as close to maximum possible in the Equation (12). The variations have been observed for the two isolation systems comprising VFPI and VCFPS for Sylmar (Northridge) and Jiji earthquakes. It is observed that on increase of damper stiffness, peak base shear, peak story drift and peak floor acceleration increase which shows that deteriorating the structural response though there is reduction in peak base displacement. The normalized peak control force increases many times as the damper stiffness increases, thus to keep damper stiffness reasonably is to maintain balance between improved structural response and limiting base displacement. Figure 3 shows the force-displacement response of the predictive controlled semiactive friction damper.

It has been learnt that on increase of damper stiffness the inclination of hysteresis loop increases which shows obvious increase in control force with decrease in damper displacement. In this study control force lower than 1000 kN is preferred so the hysteresis loop of VFPI and VCFPS can take good shape which is very essential to take the advantage of their varying curvature of sliding surfaces. For this, the damper stiffness is taken 2500 kN/m and multiplier α kept equal to 0.999.

The hysteresis loops of different control laws based on modulated homogeneous friction control algorithm for the variation of coefficient of friction (μ) in the Equations (16), (17) and (18) plotted in Figure 4. The μ has been varied from 0.09 to 0.2 for all the three cases. It has been found that as μ increases the size of hysteresis loop decreases since in the control laws based on modulated homogeneous friction, controller force is a function of peak displacement magnitude which reduces on increase of μ.

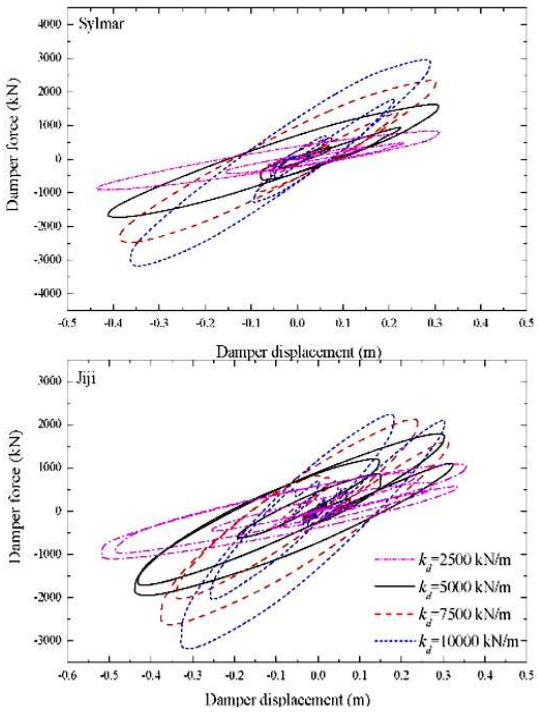

Figure 2-Hysteresis loops of predictive controlled semiactive friction damper for different damper stiffness.

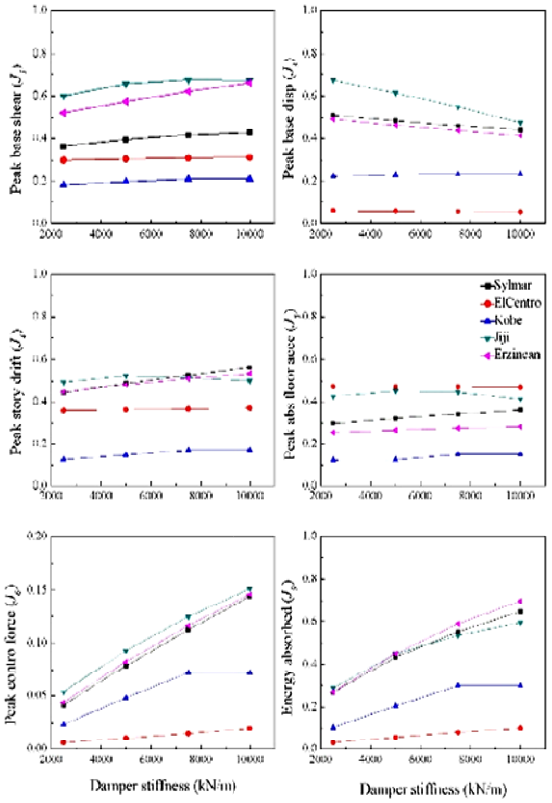

Figure 3- Effect of variation of damper stiffness of predictive controlled semiactive friction damper on evaluation criteria for different earthquakes.

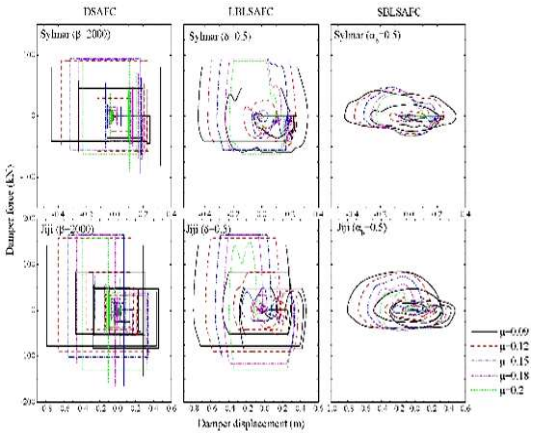

Figure 4 - Hysteresis loops of modulus homogeneous friction controlled semiactive friction dampers for different values of coefficient of friction.

In DSAFC and LBLSAFC, the areas of hysteresis loops are bigger than the SBLSAFC for both the earthquakes as the smooth variation around the boundary layer reduces the controller force thus higher increase in μ performs poor both in energy dissipation as well as structural response. The effect of variation of μ on structural response indices has been shown in Figure 5. It has been observed that on increase of μ, peak base shear, peak absolute floor acceleration and peak story drift increases and energy dissipation also reduces which is not desirable thus selection of appropriate μ is very important. For the present study the value of μ has chosen equal to 0.12.

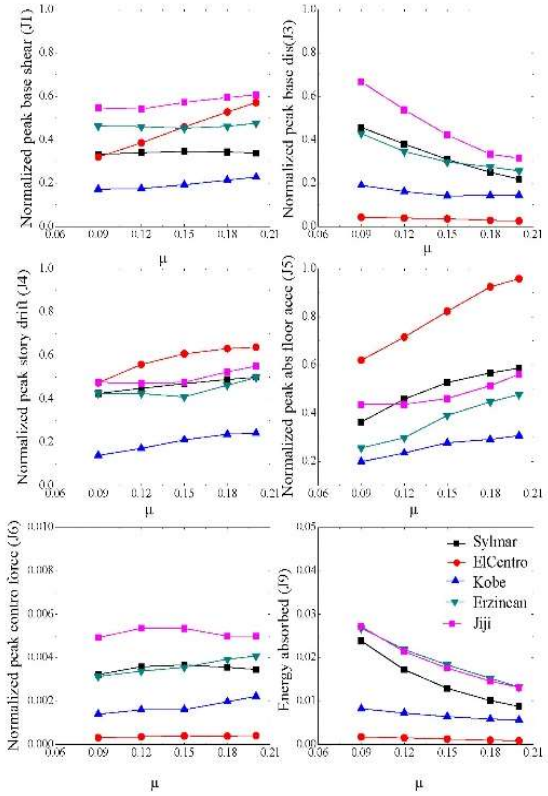

Figure 5-Effect of variation of coefficient of friction of modulus homogeneous friction controlled (LBLSAFC) semiactive friction damper on evaluation criteria for different earthquakes.

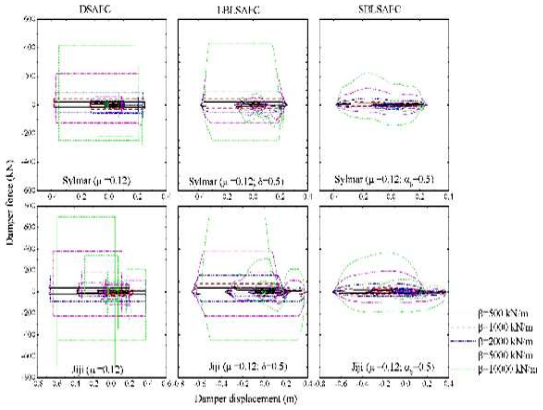

Figure 6 -Hysteresis loops of modulus homogeneous friction controlled semiactive friction dampers for different values of coefficient of positive gain.

The variation of positive gain coefficient (β) for all the control laws upon the hysteresis loop has been plotted in Figure 6, which shows that as β increases the controller force also increases but it hardly reduce the base displacement due to the fact that controllers are mostly governed by the local peak displacement signals. The above observation is equally complimented by the structural response which has been plotted in Figure 7, reflect that there is hardly any change except increase in controller force and subsequently a mild increase in energy dissipated. It concludes that higher values of β are not so productive thus selecting a reasonable value of β equal to 2000 for the present study.

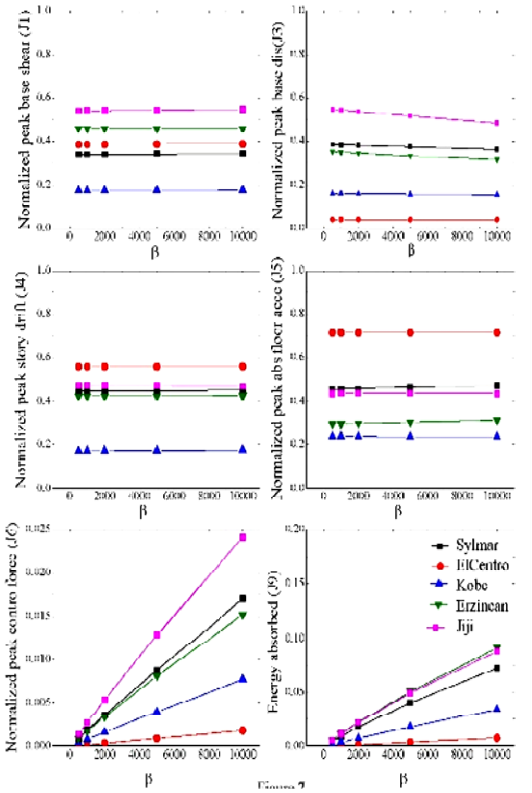

Figure 7- Effect of variation of coefficient of positive gain of modulushomogeneous friction controlled (LBLSAFC) semiactive friction damper on evaluation criteria for different earthquakes.

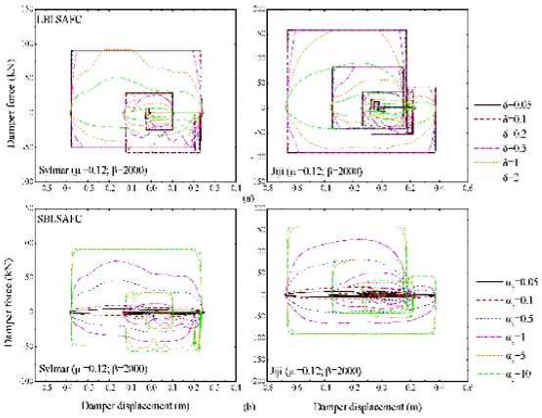

Figure 8 Hysteresis loops of modulus homogeneous friction controlled semiactive friction dampers for different values of thickness of boundary layer for LBLSAFC and SBLSAFC.

Figure 8 (a) shows the impacts of variation of thickness of boundary layer (δ) on the hysteresis loops of the semiactive friction damper. It is learnt that the effect of introducing the boundary layer is to smoothen the sharp edges in the hysteresis loop where the friction force changes in magnitude and/or sign so as avoid high frequency response of floor acceleration. It is also noted that after δ exceeds 1, the controller force decreases and the hysteresis loop shrinks which affects the energy dissipation so an appropriate value of δ chosen as 0.5. Figure 9 also reflects the same that except control force decrease after δ increases beyond 1; all other performance indices remain uninfluenced.

From Figure 8 (b) it is observed that the higher values of α turn back the smooth friction controller to discontinuous friction controller thus keeping a reasonable value equal to

0.5. Figure 10 shows that the increase of α is immaterial to structural response as the reduction in displacement is negligible except there is mild increase in control force and energy absorbed by the control devices. It can be concluded that the controller based upon modulated homogeneous friction produces small control forces such that at times it is hardly perceived any change in structural response.

The hysteresis loop is normally considered as the characteristic mechanical response of the controlling device. The hysteresis loops for the RSASD for different values of operating dampers stiffness have been plotted for two earthquakes in Figure 11 which apparently look alike as for FPS. The Figure 11 shows that as damper stiffness increases the controller force increases and damper displacement decreases, thus undue increase in damper stiffness give rise

to immense control force and subsequently poor structural performance. For the present study the damper stiffness is taken equal to 0.8 times the isolation stiffness (k_b). Figure 12 shows the variation of different performance indices with increase of damper stiffness, which confirms the above observation regarding degraded structural performance as well as inordinate increase in control forces.

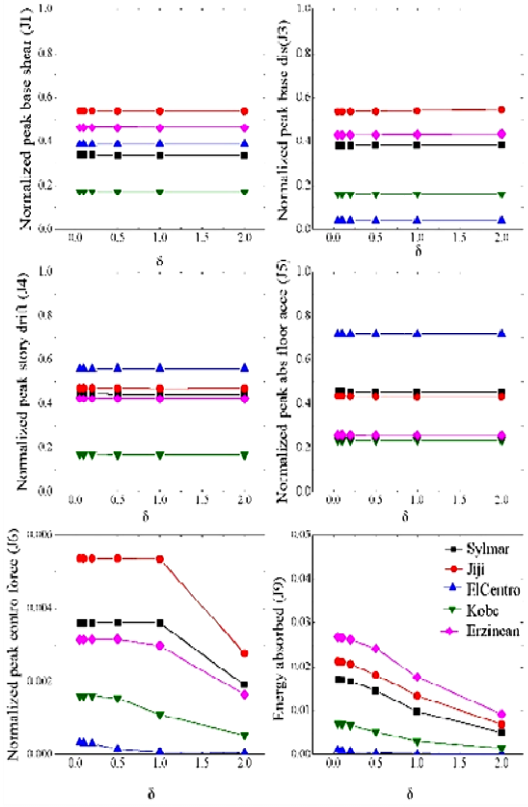

Figure 9 -Effect of variation of thickness of boundary layer of modulus homogeneous friction controlled (LBLSAFC) semiactive friction damper on evaluation criteria for different earthquakes.

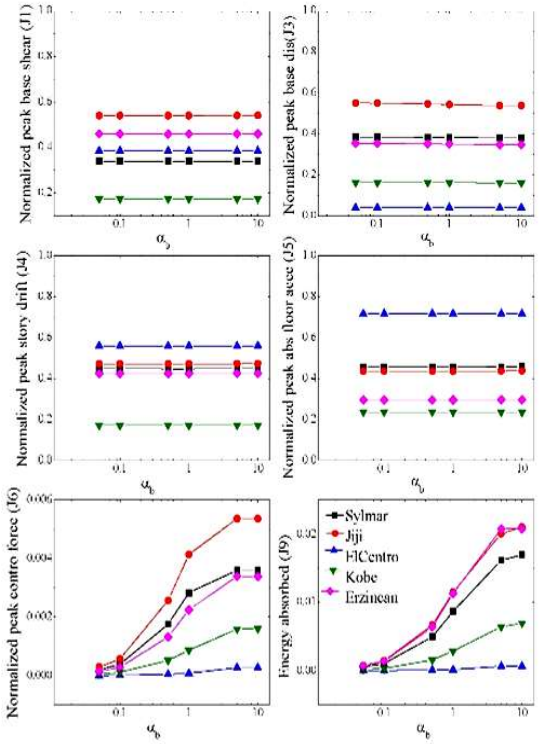

Figure 10 Effect of variation of thickness of boundary layer of modulus homogeneous friction controlled (SBLSAFC) semiactive friction damper on evaluation criteria for different earthquakes.

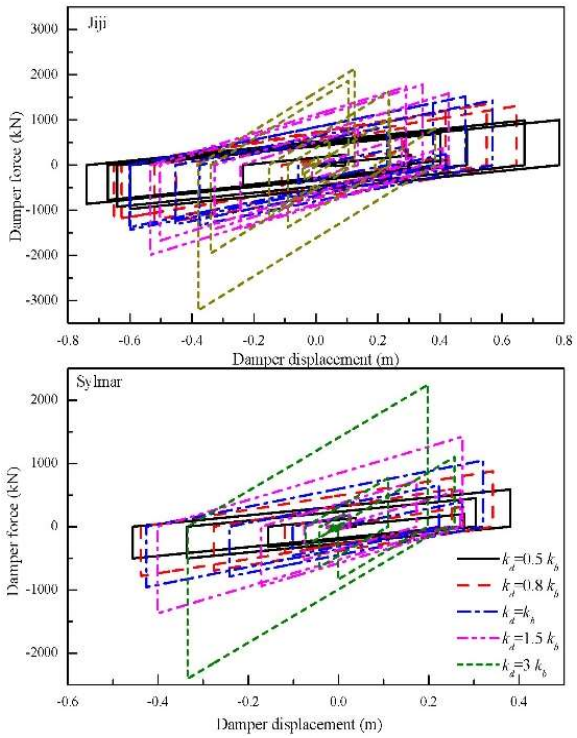

Figure 11 Hysteresis loops of resetting semiactive stiffness damper (RSASD) for different damper stiffness.

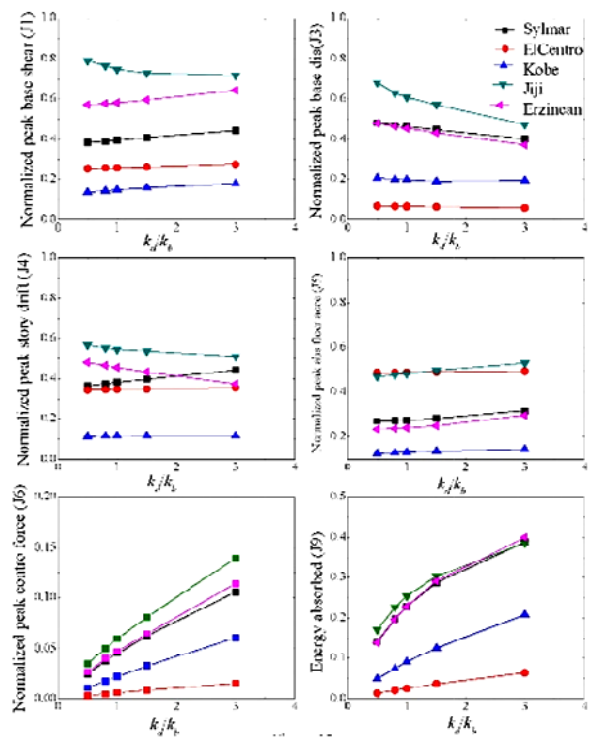

Figure 12 Effect of variation of damper stiffness of RSASD on evaluation criteria for different earthquakes.

It can be concluded from the various above observations that setting the characteristics of semiactive friction and stiffness dampers and their controllers should be done in such a way that they restrict base displacement without sacrificing much in structural response. It should also be taken care that reduction in isolator displacement especially for VFPI and VCFPS such that their hysteresis loop can take good shape otherwise these adaptive isolators remain poorly utilized. It is also found that exceptionally higher control forces are not only difficult to physically realize semi actively but also negative for structural response and at the same time very low control forces neither effective in reducing displacement nor improving structural response else proved as a cost burden to the structures. It is also experienced that different control laws governs the same semiactive damper in much different way so selection of a particular control algorithm should be done intelligently to get maximum advantage from the control device with least complications.

4.2 Comparative study of seismic response of base-isolated Irregular building with different sliding isolation systems and semiactive friction and stiffness dampers.

To know the comparative effectiveness of various isolation systems and semiactive devices the structural responses of base-isolated Irregular building isolated either with FPS or with VFPI or with VCFPS along with semiactive friction and stiffness dampers are observed. The structural responses are measured in time history records and peak values of floor accelerations; story drifts; base shears and the base displacements. All these response values are measured at the centre of the mass of the floors at respective locations in time histories both in x and y directions and compared with respective uncontrolled or simply isolated responses.All the time histories are plotted for smaller distinctive time spans just for conspicuous depiction of all the cases in spite of total time span of study is 30 sec.

Figure 13 shows the comparison of time histories of top floor absolute acceleration in x direction of base-isolated Irregular building isolated. The comparisons have been carried out for different sliding isolation systems comprising either FPS or VFPI or VCFPS and semiactive friction damper controlled with predictive control (abbreviated as “pre”); linear boundary layer semiactive friction controller (abbreviated as “MHF2”) and semiactive stiffness damper (abbreviated as “RSAS”) with respective uncontrolled values for Northridge Sylmar earthquake. The table in the right-hand sideshows the peak values of the corresponding time histories for all the semi actively controlled cases with uncontrolled values. It has been observed that for FPS isolated building, time histories of top floor acceleration for all the cases remain close to each other reflecting no increase in floor acceleration and the peak values also remain close to uncontrolled which reflect that control devices are not working efficiently with FPS. On the contrary, VFPI and VCFPS there is steep increase in the top floor accelerations which is well reflected in time histories as well as in peak values especially with MHF2. It shows that with VFPI and VCFPS these semiactive control devices decreasing the displacement thus an obvious increase in floor acceleration resulted.

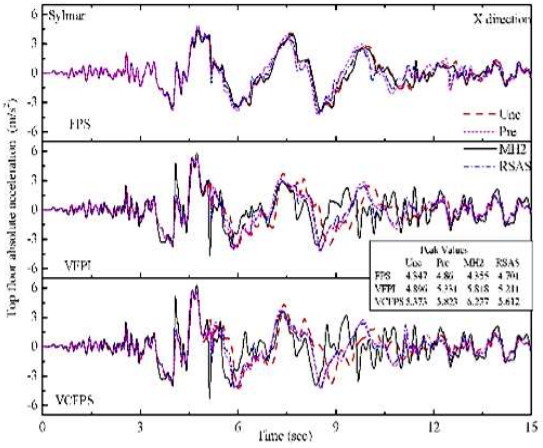

Figure 13- Time history plots of top floor absolute accelerations in x direction for base-isolated Irregular building subjected to Northridge Sylmar earthquake for different isolation systems and control devices.

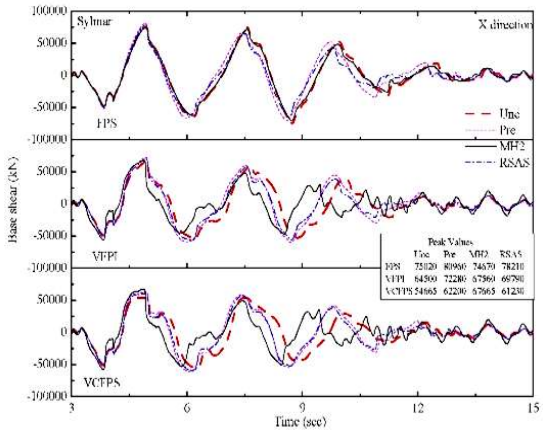

Figure 14 Time history plots of base displacement in x direction for base-isolated Irregular building subjected to Northridge Sylmar earthquake for different isolation systems and control devices.

The observations made above are well learnt from Figure 14 as well which shows the time histories plots of the base displacements in which for FPS show 6 percent maximum reduction in base displacement in controlled case whereas for VFPI and VCFPS 30 percent maximum reduction with MHF2 controlled case is observed. The reason for effectiveness of MHF2 controller with VFPI and VCFPS is that the control force is dependent of peak local displacement signals which are higher for VFPI and VCFPS and thus the controller keep constant effective control forces for longer duration and even with lower values than for FPS. The time history variation of base shear is plotted in Figure 15 which shows that VFPI and VCFPS isolated building get less base shear than FPS isolated with controlled case though there are increases in base shear than uncontrolled case which is obvious due to increase in resistance for base displacement. Similar observations regarding story drift are noted from Figure 16 which gives the time history variations of story drift for the different isolation and controlled case for the base-isolated Irregular building.

From the above observations of time histories of different structural response, it can be concluded that VFPI and VCFPS perform far better than the FPS isolation with semiactive friction and stiffness dampers. It can also be said that semiactive friction dampers control much efficiently than stiffness dampers and for them SBLSAFC based on modulated homogeneous friction control is proved better than predictive control.

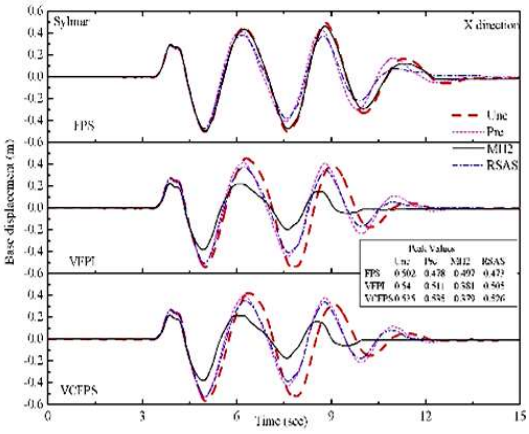

Figure 15 Time history plots of base shear in x direction for base-isolated Irregular building subjected to Northridge Sylmar earthquake for different isolation systems and control devices.

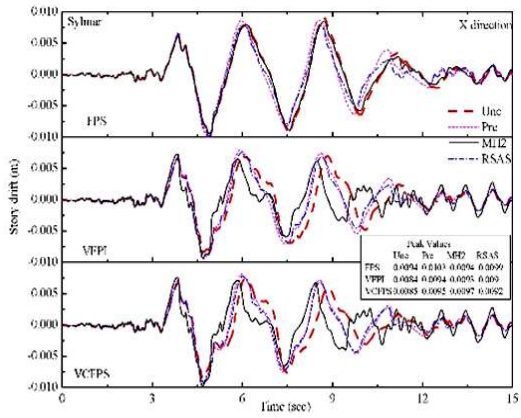

Figure 16- Time history plots of story drift in x direction for base-isolated Irregular building subjected to Northridge Sylmar earthquake for different isolation systems and control devices.

Besides the observation made over time history variations of structural response parameters, the peak values for the same have also been closely monitored for six strong near fields and one far field earthquakes mentioned earlier. The peak response values are also observed in form of normalised peak absolute floor accelerations; normalised peak base displacements; normalised peak base shears normalised; peak story drifts; normalised peak control force and normalised total energy absorbed by the controlled devices for different isolation cases with semiactive control devices. The normalization has been done by dividing the peak response values by corresponding values of non-isolated/fixed base Irregular building. Table 1 is showing normalised peak absolute floor acceleration, in which the blue and red values are corresponding minimum and maximum among the controlled values for a particular earthquake, and shaded grey represent the uncontrolled values. It is observed that from minimum 35 percent (for Rinaldi earthquake) to maximum 106 percent (for Kobe earthquake) increases from uncontrolled values have been observed in normalised peak absolute acceleration which are found with controlled VFPI and VCFPS isolated building. It has also been noticed that these acceleration increases are mostly with MHF2 controller which means that there is certain effective resistance for base/isolator displacement. Table 2 shows the peak base displacement for all the cases of isolation systems and control devices for various earthquakes. It is observed that reduction in base displacement ranges between 30-35 percent for most of the earthquakes (except 8 percent for Rinaldi earthquake) for MHF2 controlled VFPI or VCFPS isolated building. The effectiveness of VFPI or VCFPS isolation system over FPS and SBLSAFC controlled semiactive friction damper over others has been proved in time history as well as in peak response observations. In some cases, the controlled displacement increases even beyond the uncontrolled cases such in few earthquakes like Rinaldi and Kobe which is due to their typical response spectrum for displacement. The normalised peak base shears which are tabulated in Table 3 and it shows that most of the maximum values of normalised peak base shear are neither with VFPI or VCFPS isolation nor with MHF2 case controller; these are mostly associated with predictive control case. It is also observed that overall values of peak base shear of VFPI and VCFPS isolated building is much lower than FPS isolated building for strong near field earthquakes Like Jiji and Erzincan. The Table 4 displays the values of normalised story drifts for the above referred cases and it shows that peak story drifts also increase for controlled VFPI and VCFPS isolated building as peak floor accelerations for the similar reasons but for earthquakes like Jiji and Erzincan the same controlled cases found efficient and give minimum values. The normalised peak control forces for the different control and isolated cases are tabulated in Table 5, which conspicuously exhibits that the semiactive friction damper with control law MHF2 almost performs at one-tenth control force than the others for all the isolation systems. This is a bigger advantage for larger civil engineering structures because for them normally very high control forces are required which not

Table 1-Normalised peak absolute floor acceleration of base-isolated Irregular building for different isolation systems and semiactive control devices.

	Controller Type	Normalized absolute floor acceleration (J_9)						
		Newhall	Sylmar	El Centro	Rinaldi	Kobe	Jiji	Erzincan
FPS	UNCONTROLLED	0.19719	0.26588	0.48675	0.1856	0.12551	0.48674	0.22926
	PREDICTIVE	0.19968	0.27312	0.48602	0.19726	0.12924	0.47572	0.24608
	MHF2	0.19844	**0.26691**	0.48686	0.18616	0.12543	0.44776	**0.22916**
	RSAS	0.20662	0.27172	0.48874	0.19696	0.12953	**0.47809**	0.2375
VFPI	UNCONTROLLED	0.16891	0.27454	0.47502	0.15131	0.11415	0.39403	0.23626
	PREDICTIVE	**0.16979**	0.29897	0.47426	0.17072	0.12635	0.42857	0.25344
	MHF2	**0.26288**	**0.45545**	**0.71558**	0.21942	**0.23539**	0.43537	0.29505
	RSAS	0.17433	0.29223	0.47678	**0.16287**	0.12628	0.41899	0.2535
VCFPS	UNCONTROLLED	0.16824	0.30131	0.47484	0.17201	0.11528	0.49217	0.26328
	PREDICTIVE	0.17545	0.32658	**0.47408**	0.15092	0.12445	0.4395	0.27005
	MHF2	0.25349	0.43545	0.71551	**0.23249**	0.22721	0.41928	**0.32421**
	RSAS	0.17611	0.3147	0.47639	0.18335	**0.12164**	**0.41237**	0.2767

Table 2-Peak base displacement of base-isolated Irregular building for different isolation systems and semiactive control devices.

	Controller Type	Peak base displacement (J_3)						
		Newhall	Sylmar	El Centro	Rinaldi	Kobe	Jiji	Erzincan
FPS	UNCONTROLLED	0.23756	0.50179	0.06912	0.37117	0.21626	0.78836	0.50646
	PREDICTIVE	0.23635	0.47808	0.06651	0.37882	0.20293	0.67445	0.47841
	MHF2	0.23745	0.49668	**0.069**	0.37109	0.21425	**0.74821**	0.49797
	RSAS	0.23117	0.4726	0.06585	0.364	0.20138	0.62836	0.466
VFPI	UNCONTROLLED	0.2608	0.54039	0.0628	0.39189	0.21044	0.81647	0.52348
	PREDICTIVE	0.26294	0.51144	0.06001	**0.40253**	0.22364	0.67287	0.49326
	MHF2	**0.17991**	0.38128	0.0394	**0.36172**	0.16137	**0.5386**	**0.34715**
	RSAS	0.25089	0.50538	0.05987	0.37798	0.21313	0.69514	0.47702
VCFPS	UNCONTROLLED	0.27559	0.56684	0.06076	0.3879	0.22535	0.8348	0.56286
	PREDICTIVE	**0.2733**	**0.53467**	0.05833	0.40169	**0.23417**	0.72214	**0.52367**
	MHF2	0.18416	**0.3791**	**0.03933**	0.36911	**0.16131**	0.54164	0.36031
	RSAS	0.26418	0.52588	0.05798	0.37506	0.22615	0.7426	0.50596

Table 3-Normalised peak base shear of base-isolated Irregular building for different isolation systems and semiactive control devices.

	Controller Type	Normalized peak base shear (J_1)						
		Newhall	Sylmar	El Centro	Rinaldi	Kobe	Jiji	Erzincan
FPS	UNCONTROLLED	0.21487	0.37674	0.24966	0.22866	0.13291	0.83901	0.56161
	PREDICTIVE	0.22358	**0.40657**	0.26188	**0.259**	0.15002	**0.8303**	**0.60087**
	MHF2	**0.21485**	0.375	**0.24966**	**0.22865**	**0.13239**	0.80667	0.55755
	RSAS	0.21999	0.39276	0.25613	0.24222	0.14278	0.76792	0.57784
VFPI	UNCONTROLLED	0.22128	0.32391	0.29285	0.21075	0.16087	0.55425	0.46318
	PREDICTIVE	0.24688	0.363	0.29948	0.23798	0.18262	0.60057	0.52188
	MHF2	0.23951	0.33934	0.38522	0.24354	0.17487	0.5402	**0.46028**
	RSAS	0.23577	0.35051	0.29619	0.22917	0.17722	0.58947	0.50328
VCFPS	UNCONTROLLED	0.2404	0.27453	0.29568	0.2183	0.17923	0.57991	0.43428
	PREDICTIVE	**0.26553**	0.31238	0.30198	0.24501	**0.19714**	0.4919	0.48679
	MHF2	0.25509	0.33932	**0.3883**	0.25734	0.18533	0.52212	0.49032
	RSAS	0.25504	**0.30751**	0.29799	0.23982	0.19269	**0.47924**	0.48876

Table 4-Normalised peak story drift of base-isolated Irregular building for different isolation systems and semiactive control devices.

	Controller Type	Normalized story drift (J_4)						
		Newhall	Sylmar	El Centro	Rinaldi	Kobe	Jiji	Erzincan
FPS	UNCONTROLLED	0.22488	0.357	0.34525	0.17039	0.11142	0.66466	0.44273
	PREDICTIVE	0.21051	0.40222	0.34805	0.18279	0.11825	**0.68879**	**0.47778**
	MHF2	**0.22612**	**0.34706**	**0.34535**	0.17032	**0.11146**	0.63298	0.44143
	RSAS	0.22493	0.37641	0.3485	0.17697	0.11447	0.65217	0.45846
VFPI	UNCONTROLLED	0.20317	0.3989	0.35543	0.14618	0.11165	0.45635	0.40977
	PREDICTIVE	0.21588	0.44634	0.35868	0.17164	0.1288	0.49429	0.4485
	MHF2	0.21466	0.44803	0.55821	0.16404	**0.17081**	0.47124	**0.42423**
	RSAS	0.21384	0.42777	0.35866	**0.15681**	0.12266	0.48561	0.44081
VCFPS	UNCONTROLLED	0.21213	0.43504	0.35575	0.16126	0.12721	0.56601	0.44451
	PREDICTIVE	0.22364	0.47708	0.359	**0.18636**	0.14831	0.49721	0.47764
	MHF2	**0.20676**	**0.48468**	**0.55827**	0.17391	0.16059	**0.46385**	0.4618
	RSAS	0.22262	0.46255	0.35897	0.17393	0.14042	0.47426	0.4734

only require larger power sources and space to accommodate them. The Table 5 shows that VFPI and VCFPS with semiactive friction dampers controlled by MHF2 require less control forces and in earlier observations similar case earned better structural control as well. Because of lower control forces and less displacement, the energies absorbed by the control devices with VFPI and VCFPS isolated cases are observed minimum in Table 6 which records the normalised total energy absorbed by the all control devices.

Table 5-Normalised peak control force of base-isolated Irregular building for different isolation systems and semiactive control devices.

	Controller Type	Normalized Peak control force (J_6)						
		Newhall	Sylmar	El Centro	Rinaldi	Kobe	Jiji	Erzincan
FPS	PREDICTIVE	0.02558	0.04056	**0.0062**	0.03774	0.02126	**0.0561**	0.04332
	MHF2	0.00223	0.00467	0.000345	0.00354	0.00219	0.00738	0.00484
	RSAS	0.01991	0.03695	0.00467	0.03171	0.01727	0.05005	0.03908
VFPI	PREDICTIVE	0.02602	0.04153	0.00604	**0.03832**	0.0257	0.05391	0.04399
	MHF2	**0.00171**	0.0036	0.000156	**0.00347**	**0.00155**	**0.00536**	**0.0034**
	RSAS	0.02023	0.03791	0.00459	0.03188	0.01863	0.04947	0.03781
VCFPS	PREDICTIVE	**0.02616**	**0.04217**	0.0058	0.03806	**0.02446**	0.05221	**0.04511**
	MHF2	0.00175	**0.00357**	**0.000155**	0.00356	0.0016	0.00538	0.0035
	RSAS	0.02028	0.03668	0.00439	0.0315	0.01901	0.04812	0.03833

Table 6 -Normalised total energy absorbed by the control devices of base-isolated Irregular building for different isolation systems and semiactive control devices.

	Controller Type	Total Energy absorbed by controllers (J_8)						
		Newhall	Sylmar	El Centro	Rinaldi	Kobe	Jiji	Erzincan
FPS	PREDICTIVE	0.1145	0.26114	0.03103	0.2046	0.10111	**0.30334**	0.26285
	MHF2	0.01375	0.05452	0.0015	0.03396	0.0138	0.07456	0.05201
	RSAS	0.07662	0.19807	0.02059	0.14897	0.07413	0.2264	0.19698
VFPI	PREDICTIVE	0.11679	**0.26664**	**0.03132**	0.20711	0.10495	0.28664	**0.2692**
	MHF2	**0.00546**	0.01453	0.000314	**0.01254**	**0.00536**	0.01821	0.01916
	RSAS	0.08299	0.19851	0.02211	0.15098	0.07685	0.20626	0.20151
VCFPS	PREDICTIVE	**0.11679**	0.25506	0.03068	**0.217**	**0.109**	0.24588	0.25218
	MHF2	0.00563	**0.01366**	**0.000311**	0.01335	0.00551	**0.01615**	**0.01816**
	RSAS	0.08439	0.18962	0.02181	0.15759	0.07957	0.18154	0.19133

From the observation of normalised peak structural response it can be concluded that the base-isolated Irregular building isolated with VFPI and VCFPS with control devices perform much better than FPS isolated. It can also be resolved that semiactive electromagnetic friction damper controlled with law based on modulated homogeneous friction with boundary layer proved better control device in comparison to others.

5. CONCLUSIONS

The seismic control of base-isolated Irregular building which is under the action of strong earthquakes acting bi-directionally is exercised through ERB and FPS or VFPI or VCFPS with semiactive friction or stiffness control devices. The influences of variation of characteristics of semiactive control devices on their force displacement behaviors and structural response of base-isolated Irregular building are investigated. The comparative performances of different isolation systems and semiactive control devices are observed on the base-isolated Irregular building. From the trends of the observed results in form of evaluation criteria, the following conclusions can be made.

1. The appropriate selection of mechanical characteristics of semiactive dampers and key parameters of control laws are vital for their efficient performance. The optimum values not only govern the magnitude of control forces but also good shape of their hysteresis loop enable them for adequate energy dissipation and ensure better structural response.
2. Higher values of damper stiffness gives higher control forces and which leads to poor structural response for predictive controlled semiactive friction damper and RSASD.
3. The higher values of coefficient of friction and positive gain coefficient for control laws based on modulated homogeneous friction give higher control forces which deteriorates the structural response.
4. Higher values of the thickness of linear boundary layer for LBLSAFC reduce the control forces substantially such that damper becomes almost ineffective. Similarly,

higher values of thickness of smooth boundary layer for SBLSAFC bring back it to discontinuous control and add high frequency input to floor accelerations.

5. The VFPI and VCFPS based isolation systems perform better than the FPS based isolation system with semiactive control devices especially under strong near field earthquakes.

6. Semiactive electromagnetic friction damper controlled by law based on modulus homogeneous friction works efficiently with VFPI and VCFPS isolation systems. It not only functions with lower control forces but also restricts base displacement with lower base shear and story drift for strong near field earthquakes.

Disclosures

Free Access to this article is sponsored by SARL ALPHA CRISTO INDUSTRIAL.

7. REFERENCES

[1] Kawashima K et al. Effectiveness of the variable damper for reducing seismic response of highway bridges against earthquakes. In: Proc. 2nd US–Japan Workshop on earthquake protective system for bridges. Tsukuba (Japan): PWRI, 1992:479–94.

[2] Kawashima K, Unjoh S, Shimizu K. Experiments on dynamics characteristics of variable damper. Proc Japan Nat Symp on Struct Response Control 1992;121.

[3] Yang JN, Li Z, Wu JC, Kawashima K. (1994a), Aseismic hybrid control of bridge structures. In: Proc 5th Natl Conf on Earthquake Engng, Chicago, IL, 1994;1:861–70.

[4] Yang JN, Wu JC, Kawashima K, Unjoh S. Hybrid control of seismic-excited bridge structures. J Earthquake Engng Struct Dynam 1995;24(11):1437–51.

[5] Kobori T, Takahashi M, Nasu T, Niwa N, Ogasawara K. Seismic response controlled structure with active variable stiffness system. J Earthquake Engng Struct Dynam 1993;22:925–41.

[6] Kamagata S, Kobori T. Autonomous adaptive control of active variable stiffness systems for seismic ground motion. In: Proc. First World Conference on Structural Control, 2, TA4-23, Pasadena (CA). Los Angles: USC, 1994.

[7] Yang JN, Wu JC, Li Z. Control of seismic-excited buildings using active variable stiffness systems. J Engng Struct 1996;18(8):589–96.

[8] Gavin HP, Hanson RD, Filisko FE. Electroheological dampers, Part I: analysis and design. J Appl Mech ASME 1996;63(3):669–75.

[9] Gavin HP, Hanson RD, Filisko FE. Electroheological dampers, Part II: testing and modeling. J Appl Mech ASME 1996;63(3):676–82.

[10] Spencer BF Jr., Dyke SJ, Sain MK, Carlson JD. Phenomenological model of a magnetorheological damper. J Engng Mech ASCE 1997;123(3):230–8.

[11] Spencer BF, Jr, Carlson JD, Sain MK, Yang G. On the current status of magnetorheological dampers: seismic protection of full scale structures. In: Proc American Control Conference, Albuquerque, NM, 1997:p. 458–62.

[12] Spencer BF Jr., Sain MK. Controlling buildings: a new frontier in feedback. IEEE Control Systems 1997;17(6):19–35.

[13] Nagarajaiah S, Mate D. Semi-active control of continuously variable stiffness system. In: Proc 2nd World Conf on Structural Control, vol. 1. New York: Wiley, 1998:397–406.

[14] Nagarajaiah S, Mate D. Development of a semi-active continuously variable stiffness device. In: Proc ASCE, 12th Engng Mech Conf. Reston, VA: ASCE, 1998:257–60.

[15] Yang JN, Kim JH, Agrawal AK. Seismic response control using semi-active stiffness dampers. In: Proc Int Workshop on Seismic Isolation, Energy Dissipation and Control of Structures. Guangzhou, China: Seismological Press, 1999:312–9.

[16] Yang JN, Kim JH, Agrawal AK. A resetting semi-active stiffness damper for seismic response control. J Struct Engng ASCE 2000;126(12):1427–33.

[17] Bobrow JE, Jabbari F, Thai K. A new approach to shock isolation and vibration suppression using a resetable actuator. J Dynam Syst Measur Control ASME 2000;122:570–3.

[18] Fujita T et al. Semiactive seismic isolation using controllable friction damper. Bull Earthq Resistant Structure Res Center 1994;27(2):21–31.

[19] Akbay Z, Aktan HM. Abating earthquake effects on buildings by active slip brace devices. Shock and Vibration 1995; 2:133–42.

[20] Dowdell DJ, Cherry S. Semi-active friction dampers for seismic response control of structures. Proc 5th US National Conf Earthquake Engng 1994;1:819–28.

[21] Inaudi JA. Modulated homogeneous friction: a semi-active damping strategy. J Earthquake Engng Struct Dynam 1997;26:361–76.

[22] Agrawal AK, Yang JN. A semi-active hybrid isolation system for buildings subject to near-field earthquakes. In: Advanced Technology in Structural Engineering, CD RAM, 8 pp., ASCE, Proc ASCE 2000 Structures Congress and Exposition, Philadelphia (PA), 2000.

[23] Agrawal AK, Yang JN. A semi-active electromagnetic friction damper for response control of structures. In: Advanced Technology in Structural Engineering, CD RAM, 8 pp., ASCE, Proc ASCE 2000 Structures Congress and Exposition, Philadelphia (PA), 2000.

[24] Reinhorn AM, Soong TT, Yen CY. Base-isolated structures with active control. Rec Adv Design Analy Test Qualif Meth PVP ASMA 1987;127:413–9.

[25] Yang JN, Danielians A. Aseismic hybrid control systems for building structures. J Engng Mech ASCE 1991;117(4):836–53.

[26] Yang JN, Li Z, Liu SC. Control of hysteretic system using velocity and acceleration feedbacks. J Engng Mech ASCE 1992;118(11):2227–45.

[27] Yang JN, Li Z, Danielians A. Hybrid control of nonlinear and hysteretic systems II. J Engng Mech ASCE 1992;118(7):1441– 56.

[28] Yang JN, Li Z, Vongchavalitkul S. A generalization of optimal control theory: linear and nonlinear control. J Engng Mech ASCE 1994;120(2):266–83.

[29] Yang JN, Li Z, Vongchavalitkul S. Stochastic hybrid control of hysteretic structures. J Prob Engng Mech 1994;9:125–33.

[30] Nagarajaiah SM, Riley MA, Reinhorn AM. Hybrid control of sliding isolated bridges. J Engng Mech ASCE 1993;119:2317–32.

[31] Yang JN, Li Z, Wu JC, Hsu IR. Control of sliding-isolated buildings using dynamic linearization. J Engng Struct 1994;16(6):437–44.

[32] Yang JN, Wu JC, AgrawalAK, Li Z. Sliding mode control for seismic-excited linear and nonlinear civil engineering structures. NationalCenter For Earthquake Engineering Research, Technical Report NCEER-94-0017, 1994.

[33] Yang JN, Wu JC, Agrawal AK. Sliding mode control of nonlinear and hysteretic structures. J Engng Mech ASCE 1995;121(12):1386–90.

[34] Yang JN, Wu JC, Reinhorn AM, Riley M. Control of sliding isolated buildings using sliding mode control. J Struct Engng ASCE 1996;122(2):83–91.

[35] Yang JN, AgrawalAK, Chen S. Optimal polynomial control of seismically excited non-linear and hysteric structures. J Earthquake Engng Struct Dynam 1996;25(11):1211–30.

[36] Nagarajaiah S. Fuzzy controller for structures with hybrid isolation system. In: Proc First World Conf on Structural Control, University of Southern California, CA, TA2-67-76, 1994.

[37] Symans MD, Kelly SW. Fuzzy logic control of a seismically isolated bridge structure. J Earthquake Engng Struct Dynam 1999;28(1):37–60.

[38] Agrawal AK, Yang JN. A semi-active control strategies for buildings subject to near-field earthquakes. In: Smart structures and materials 2000: Smart systems for bridges, structures and highways, Proc. SPIE, 3988, 2000:359–70.

[39] Johnson EA, Ramallo JC, Spencer BF, Sain MK. Intelligent base isolation systems. In: Proc Second World Conf on Structural Control, Kyoto (Japan), vol. 1. New York: Wiley, 1998:367–76.

[40] Sahasrabudhe S, Nagarajaiah S. Sliding isolated structures with smart dampers. In: Proc Int Conf on Advances in Structural Dynamics, Hong Kong, CD ROM, 2000.

[41] Nagarajaiah S, Sahasrabudhe S, Iyer R. Earthquake protection of bridges using sliding isolation system and MR dampers. In: Proc Third Int Workshop on Structural Control. Paris: ENPC, 2000:375–83.

[42] Yang JN, Agrawal AK. Protective system technology for building structures against near-field earthquakes. In: Proc Int Workshop on Annual Commemoration of Chi-Chi earthquake, vol. II—technology aspect. Taipei, Taiwan: NationalCenter for Research on

Earthquake Engineering, 2000:76–87.

[43] Yang JN, AgrawalAK, He W. Response control of nonlinear structures using a semi-active stiffness damper. In: Advances in structural dynamics, vol. I, Proceedings of International Conference on Advances in Structural Dynamics. Oxford: Elsevier Science, 2000:349–56.

[44] Nagarajaiah S, Sahasrabudhe S, Iyer R. Seismic response of sliding isolated bridges with smart dampers subjected to near source ground motions. In: Proc Structures Congress, ASCE, Philadelphia, CD ROM, 2000.

[45] Sahasrabudhe S, Nagarajaiah S, Hard C. Experimental study of sliding isolated buildings with smart dampers subjected to near source ground motions. In: Proc Engng Mech Conf EM 2000, ASCE, UT Austin, CD ROM, 2000.